

A Modeling Technique for Precast Concrete Frames with Hybrid Connections

Andrei Faur^{*1}, Călin Mircea², Mircea Păstrav³

^{1,2} *Technical University of Cluj-Napoca, Faculty of Civil Engineering. 15 C Daicoviciu Str., 400020, Cluj-Napoca, Romania*

³ *National Institute for Research & Development in Construction and Economy of Construction, Cluj-Napoca Branch. 117 Calea Florești Str., 400524, Cluj-Napoca, Romania*

Received 15 September 2012; Accepted 5 November 2012

Abstract

The paper describes a modeling technique that can be used in various finite element based software products to facilitate the modeling and design of hybrid frame connections. The complex behavior of an interior beam-column sub-assembly is counteracted using frame elements with fiber hinges, nonlinear springs and cable objects. An analytical model is compared with a full scale, hybrid frame connection specimen that has been tested to a displacement controlled cyclic loading sequence. The monotonic behavior is investigated, as well as the performance when subjected to a one-cycle enforced displacement sequence up to the maximum drifts considered in design.

Rezumat

Lucrarea descrie o tehnică de modelare numerică, care poate fi implementată în diverse produse software de element finit, pentru a facilita procesele de calcul a cadrelor prefabricate de beton armat cu îmbinări hibride. Comportarea complexă a unui subansamblu interior de grindă-stâlp este surprinsă cu ajutorul elementelor liniare unidimensionale cu posibilitate de plastifiere concentrată la nivel de fibră, a elementelor de legătură de tip resort neliniar și a elementelor de tip cablu. Un model analitic este comparat cu un specimen experimental de îmbinare hibridă, conceput la scară naturală, care a fost testat la o secvență de încărcare ciclică, controlată în deplasări. Este investigată comportarea la solicitări monotone și, de asemenea, performanța îmbinării când este supusă unui singur ciclu de încărcare-descărcare prin care se impune atingerea deplasărilor maxime considerate la dimensionare.

Keywords: hybrid connections, post-tensioning, special reinforcement, frame elements with fiber hinges, cable elements, multi-linear plastic link elements.

1. Introduction

The need for an efficient precast concrete frame system to be built in areas of high seismicity led to the development of the so-called hybrid frame connections (HFC). This type of connections make

*Corresponding author: Tel./ Fax.: +40 264 40 15 45
E-mail address: Andrei.FAUR@dst.utcluj.ro

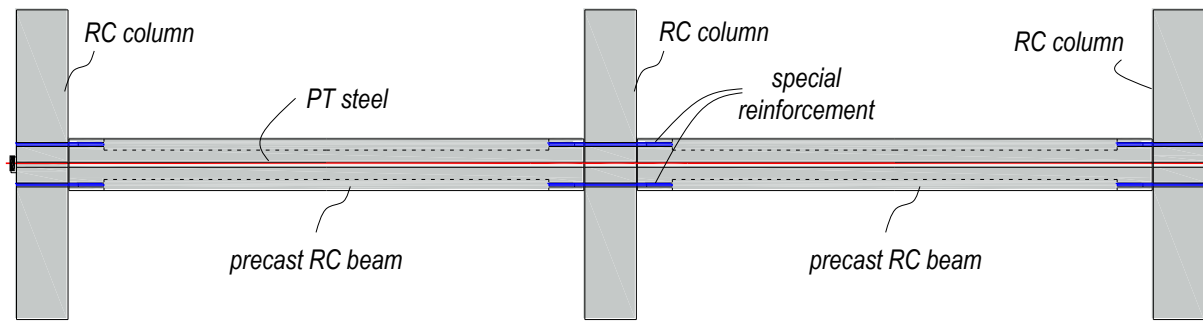


Figure 1. Example of a single-level hybrid frame system.

use of post-tensioned (PT) strands and partially unbounded mild steel rebars as assembly devices for the prefabricated frame units. In fact, the hybrid frame system (HFS) consists of multi-level cast-in-place concrete columns between which multiple single-bay precast concrete beams are erected and fixed through post-tensioning (Fig. 1). The HFC concept was developed during an experimental program conducted at the National Institute of Standards and Technology (NIST) [1] and the PRESSS research program [2].

The post-tensioned strands are placed into polyethylene ducts and pass in a straight line through the columns and through the mid-depth of the beams. Thus, the post-tensioning effect can be transmitted simultaneously to several frame units (Fig. 1). Due to the post-tensioning effect, friction is created at the beam-column interface and the required shear resistance is ensured. Once the gap at the beam-column interface opens, the post-tensioning also generates a clamping force that endows the HFS with self-centering capabilities. No seismic energy is dissipated by the PT steel because it is designed to remain elastic during the whole loading-unloading sequence.

The mild steel rebars are individually introduced into steel ducts which are already placed at the top and bottom of both beam ends (Fig. 1). A fiber reinforced grout is used to bond each reinforcing bar to the steel duct, but a short length near the beam-column interface is intentionally left without any bond. The reason is to delay the fracture of the mild steel rebars as they act as energy dissipaters and contribute along with the PT steel to the overall bending moment capacity of the connection. Such a type of reinforcement is known as special reinforcement (SR).

In terms of seismic performance, a hybrid frame system is competitive with any other monolithic frame structure. Besides that, it benefits from two unique abilities regarding the post-quake behavior. The first one was mentioned earlier and refers to the ability of the connection to bring the whole framing system back to its original un-deformed state (i.e., all residual deformations tend to minimum), while the second one regards the capacity to maintain the precast frame units at a fully operational level. This is achieved by concentrating the most significant earthquake-induced damages at the beam-column interfaces.

Despite all of the benefits provided by the PT steel and the SR, modeling the HFS with commonly used FEM analysis programs proved to be a very difficult task and only few attempts have been made in this direction [3,4]. Hawileh et al. [3] proposed a three-dimensional nonlinear finite element model using ANSYS 8.0, while Balica [4] managed to capture the gap opening at the beam-column interface through the use of multiple link elements. In the last mentioned study, SAP2000 analysis program was used to define the analytical model. However, the major drawback lies in the existence of the SR unbounded length which makes the plain section hypothesis no longer valid in the region near to the beam-column interface.

2. Research significance

A simple and efficient modeling approach is needed for nonlinear analyses of precast frame-to-

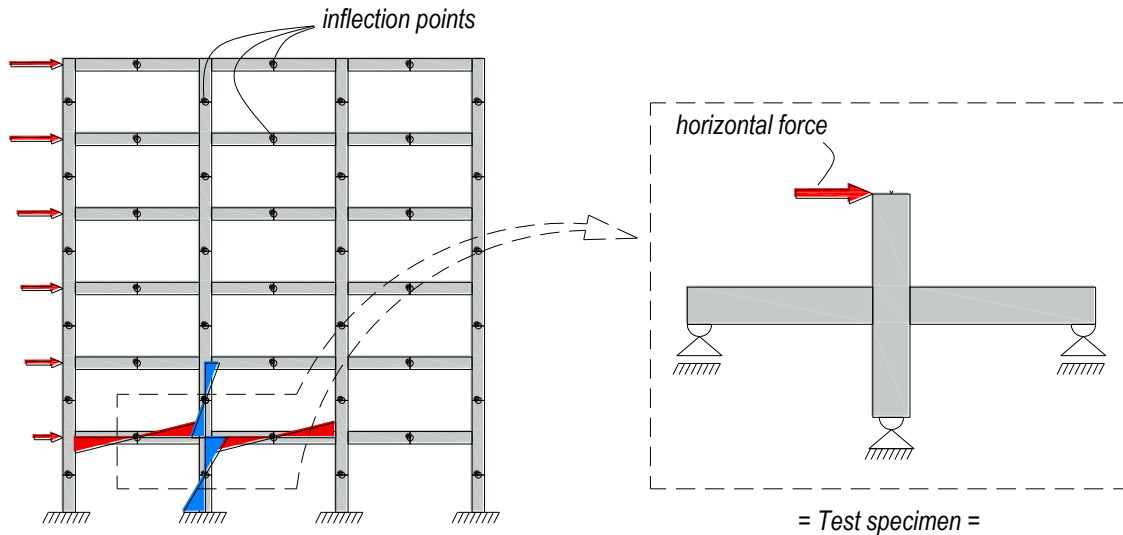


Figure 2. Locating the test specimen in the real structure.

column subassemblies with HFC. From the designer's perspective, it is very important to predict the displacement capacity of the connection, as accurate as possible, without any testing or sophisticated FEM analyses. Moreover, a proper evaluation of the cyclic behavior may even eliminate the necessity of cyclic analyses. The present study addresses the above-mentioned concerns and proposes an analytical model for a test specimen which was part of an experimental research program conducted at INCERC Cluj-Napoca.

3. Testing program

3.1 Specimen detailing and design

A full scale specimen consisting in an interior beam-column joint was tested to a displacement controlled cyclic loading sequence. The joint was considered to be located at the first level of a six story hybrid frame building, and contains the frame parts between two subsequent inflection points (i.e., a 3.00m length column and two half-length beams of 2.50m length), as shown in Fig. 2. The

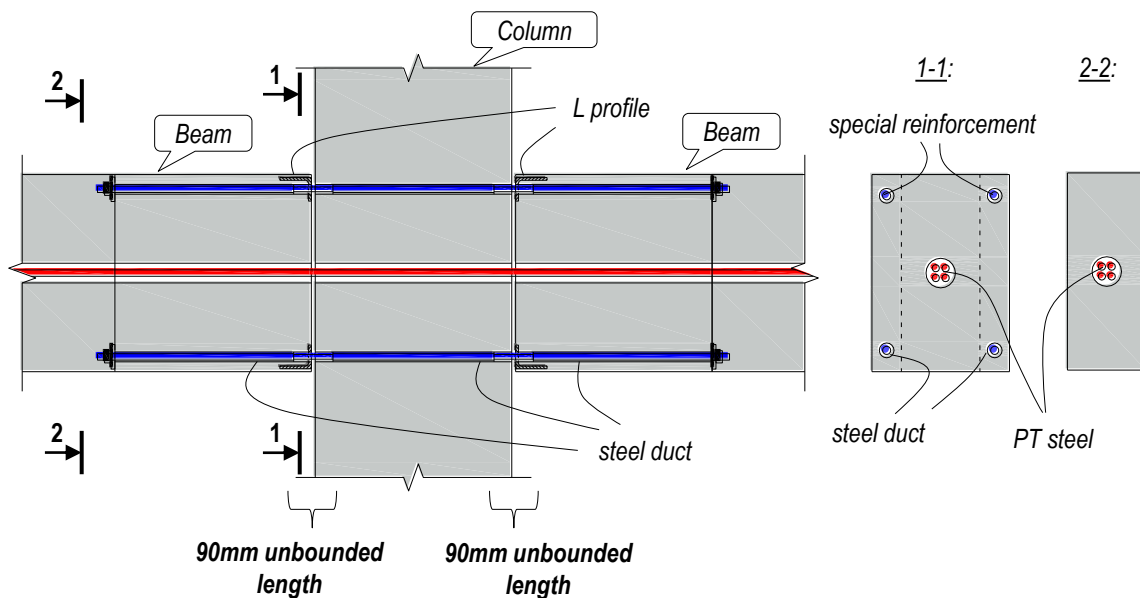


Figure 3. The connection detail.

specimen was designed to withstand a maximum drift of 0.025 under the conditions imposed by a seismic region with a design ground acceleration of 0.24g and a corner period of 0.1sec. For the design purpose, the *Direct Displacement Based Design* (DDBD) [5] method was used to find the forces at the connection (i.e. the beam-column interface) and, with the use of ACI T1.2-03 [6] guidelines, the proper amounts of PT steel and SR were established. 70% of the total moment capacity of the connection is taken by the PT steel, while the rest of 30% is taken by the special reinforcement. The DDBD steps and results were presented in detail in [7]. The connection detail obtained from the design can be seen in Fig. 3.

Four mild reinforcing bars of 12mm in diameter were grouted into steel ducts. A 90mm unbounded length was considered for each rebar at the beam-column interface. The bars act as special reinforcement and are placed symmetrically with respect to the beam mid-depth (Fig. 3). The steel used has a yield tensile strength of 345MPa and an ultimate strength 510MPa. The PT steel is consisted in four 12.5mm strands made of high strength steel, with 1636MPa yielding stress and 1860MPa ultimate strength [7].

A total of 42 complete loading-unloading cycles were applied to the testing specimen. An imposed horizontal displacement of the column's top-end was used to obtain the target drift values. To reach the maximum drift, the displacement was gradually increased at every three cycles, starting from zero and reaching to 75mm (i.e. the corresponding value for the relative drift of 0.025). Basically, the test followed the procedure used at NIST for the Phase IV specimens [1].

3.2 Test observations and results

The testing specimen performed well at the imposed displacements, showing a typical hybrid frame connection behavior. Only a few damages consisting in unclosed cracks were observed at the end of the testing procedure, most of them being located at the beam-column interfaces. Due to the self-centering effect, the prefabricated frame units (i.e. the two beams and the column) remained in a very good condition and it is assumed that only elastic deformations were encountered by the frame elements. No shear slip and no spalling of concrete cover were observed at the beam ends that are in contact with the column faces.

The main purpose of the testing program was to obtain the hysteresis curves (i.e. the force-displacement cyclic curves). Based on these results it was possible to get the envelope curves, and then to estimate the initial stiffness and the residual displacement for both positive and negative

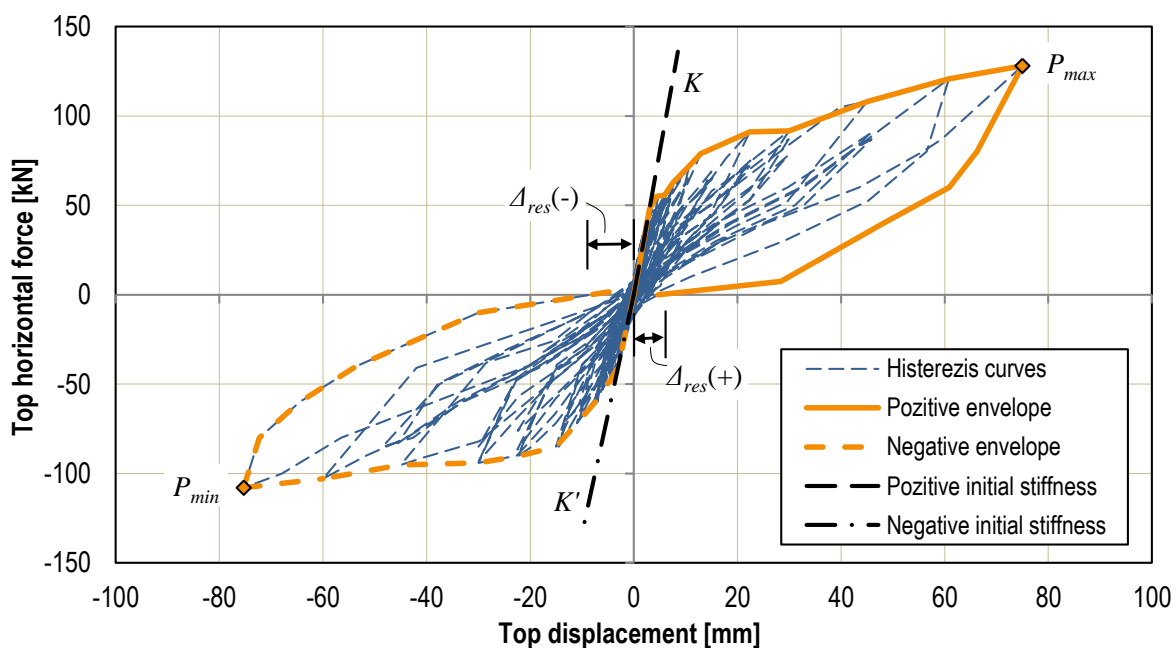


Figure 4. Test results.

loadings. All are shown in Fig. 4, where: P_{max} and P_{min} – horizontal forces associated with the positive and negative maximum drifts, respectively; K and K' – initial stiffness for both positive and negative loading; $\Delta_{res}(+)$ and $\Delta_{res}(-)$ – residual displacements obtained from the positive and negative envelope curves, respectively. Table 1 contains the values of the terms mentioned above.

Table 1: Horizontal forces, initial stiffness and residual displacements test results

| Test result | Unit of measurement | Value |
|-------------------|---------------------|---------|
| P_{max} | [kN] | 128.00 |
| P_{min} | [kN] | -108.00 |
| K | [kN/mm] | 16.00 |
| K' | [kN/mm] | 13.33 |
| $\Delta_{res}(+)$ | [mm] | 4.70 |
| $\Delta_{res}(-)$ | [mm] | -8.40 |

4. Analytical Model

The analytical model presumes the use of fiber frames (i.e., frame elements with fiber hinges) and nonlinear link elements. SAP2000 is a widely used structural analysis program that benefits of these features and therefore was used to model the specimen’s behavior.

The same boundary conditions depicted in Fig. 2 for the interior beam-column sub-assembly are applied to the analytical model. The column is pinned at the bottom with a hinge restraint, while both beam ends that are not in contact with the column faces are pinned with roller restraints. A restraint for blocking only the horizontal displacement is assigned to the joint located at the column’s top end in order to impose a ground displacement loading pattern (Fig. 5). In this manner, any enforced displacement history can be applied to generate the force-displacement curves.

Two monotonic loading sequences were considered in the analysis. The first one gradually increases the column’s top end displacement, starting from zero to the positive maximum drift (i.e. +75mm), while the second loading sequence gradually enforces the column’s top end to reach both positive and negative maximum drifts, in the following order: from zero displacement, to the positive maximum drift, then to the negative maximum drift (i.e. -75mm), and finally back to zero.

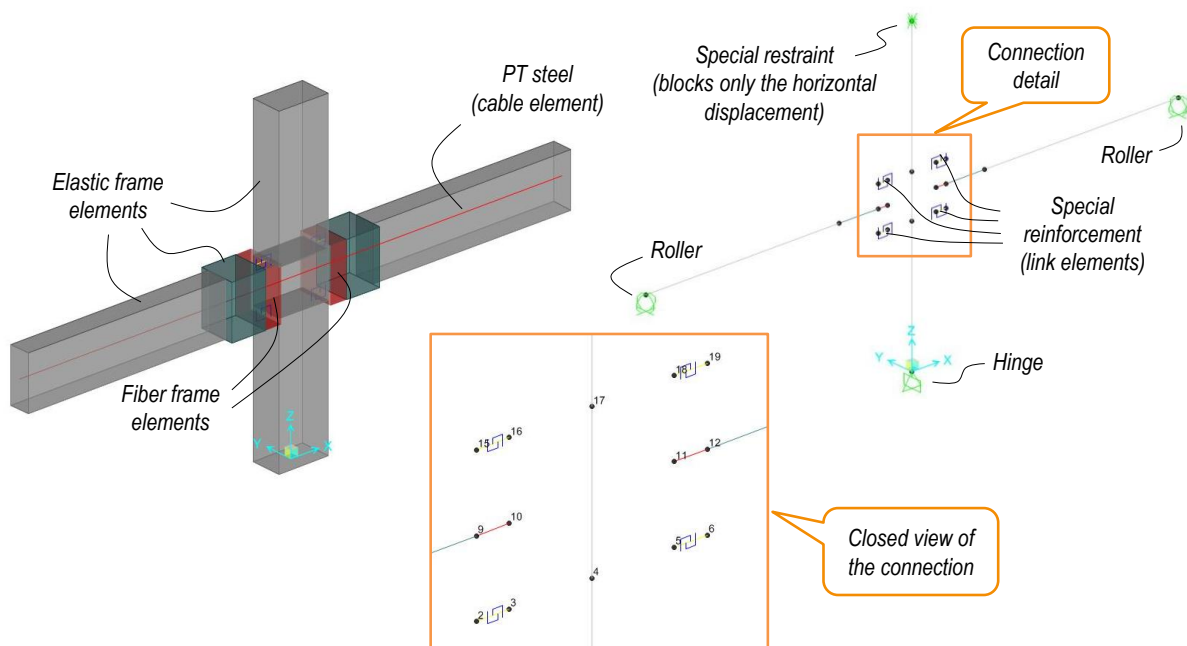


Figure 5. Analytical model.

The monotonic and the cyclic force-displacement curves obtained can be compared with the test envelope curves shown in Fig. 4.

4.1 Modeling the precast frame units

Given that only minor cracks were identified along the precast frame units, was assumed that the two beams and the column behaved elastic during the whole testing procedure. Therefore, the column is modeled entirely with elastic frame elements, as well as the beams, except for the regions where the SR is intentionally unbounded. Under the unbounded length the beams are modeled with fiber frame elements (Fig. 5).

The beam ends that are in contact with the column faces are made wider to facilitate the access to the SR bars [7]. This modification is justified only by technological reasons and it is not meant to change the behavior of the connection. On the other hand, it requires two elastic frame elements, with different cross-sectional geometries in order to complete the beam model. The three element models (i.e., two elastic frame elements and one fiber frame element) are shown in Fig. 5.

4.2 Modeling the PT steel

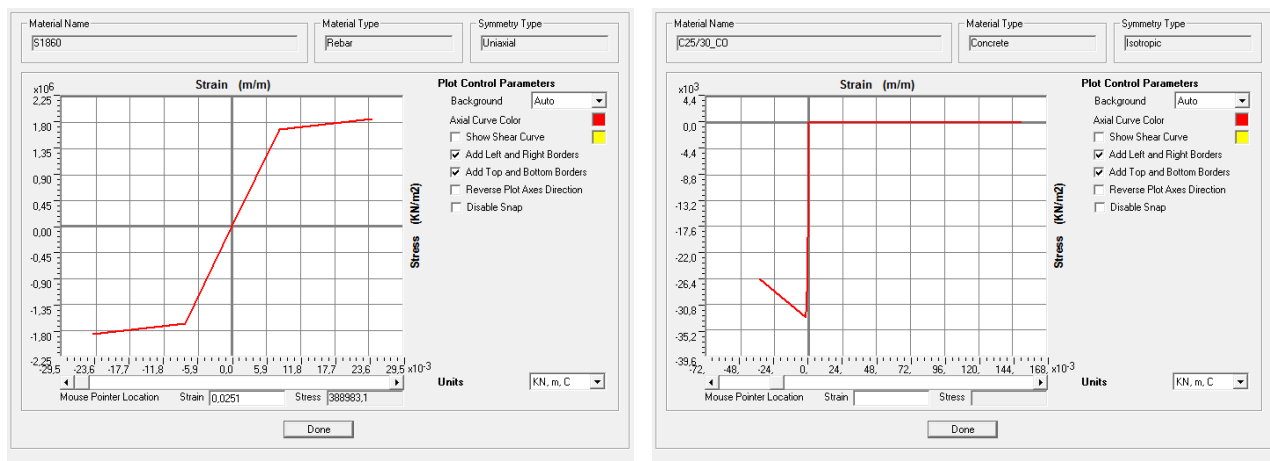
Cable elements are used to model the PT steel. Even though SAP2000 benefits by a special object (namely the tendon object) to represent the effect of post-tensioning [8], it was considered that through the use of cable elements, the analytical model proposed herein gains a wider application range. The vast majority of structural analysis programs have the option to make use of cable elements.

The mechanical characteristics of the PT strands are considered through the material properties defined for the cable element. In this case, an uniaxial material with a bilinear constitutive law is defined, heaving the stress-strain curve presented in Fig. 6(a).

4.3 Modeling the special reinforcement

The special reinforcement is modeled with Multi-Linear Plastic link elements. This type of link element considers a kinematic hardening behavior for uniaxial deformation [8]. It is also suitable for cyclic analysis.

The analysis takes into account only the in-plane deformations of the frame sub-assembly. Therefore, four link elements were needed to model the SR bars over the unbounded length (i.e., each link element has the length equal to the unbounded length of the SR bars). The location of



(a)

(b)

Figure 6. Material stress-strain curves for cable elements (a) and concrete fibers (b).

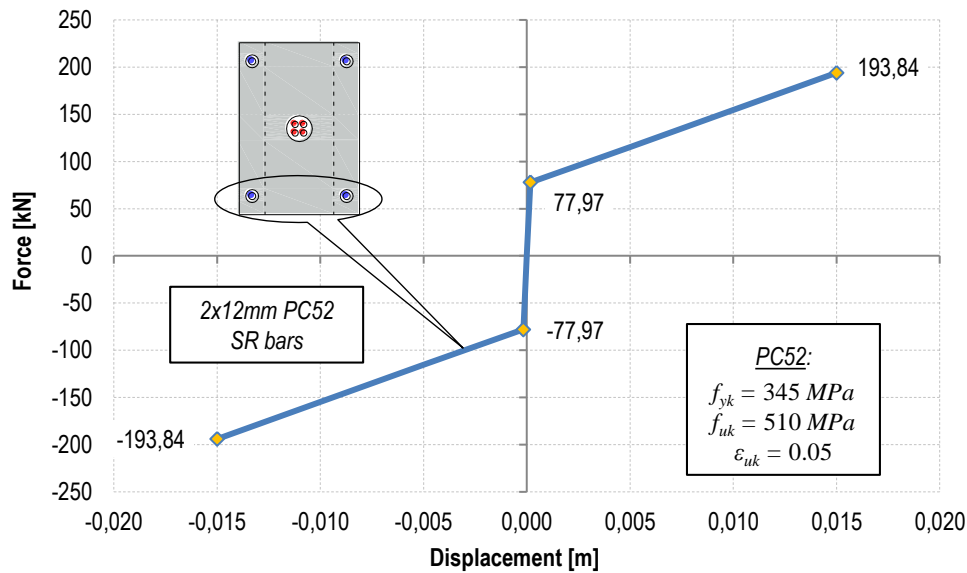


Figure 7. Force-displacement curve of the link elements.

each link element is shown in Fig. 5, and it can be seen that only one link element is needed to model the SR bars that share the same vertical position over the cross-sectional beam height. Only the properties in the longitudinal direction are considered for the link elements, meaning that the SR bars are able to support only uniaxial deformations. The mechanical characteristics are defined through the force-displacement curve from Fig. 7, which implies the estimation of the maximum elongation and the maximum axial force encountered in each pair of SR bars (i.e., the SR bars that are modeled through a single link element). The gap opening at the beam-column interface was measured during the test at the location of the SR bars, and it never exceeded 12mm . Therefore, the force-displacement curve for the link elements presented in Fig. 7 is constructed for a maximum displacement of 15mm .

4.4 Modeling of beam-column interface

The beam ends that are in contact with the column faces present a nonlinear behavior only over the length where the SR is unbounded. This specific beam region is modeled with a fiber frame element with a single fiber hinge in the middle. The hinge length is equal to the frame's length (i.e. the unbounded length of the SR) and every hinge consists in 50 concrete fibers which are evenly spread over the cross-sectional height. Only the concrete contribution is considered in the analysis.

To model the gap opening at the beam-column interface, the modification proposed by El-Sheikh et al. [9] is made to the concrete uniaxial model for neglecting the tensile stiffness and strength. The material stress-strain curve used for the concrete fibers is built to reach a maximum tensile deformation of 15mm and it is shown in Fig. 6(b).

Both fiber frame elements are tied to their adjacent link elements by rigid links. In SAP2000 this is done by assigning joint constraints to the nodes expected to have a rigid-body behavior. In the present case, body constraints (i.e., rigid-body joint constraint type) were applied to three sets of joints, as follows (Fig. 5): joints 2, 9 and 15 – first body constraint; joints 3, 4, 5, 10, 11, 13, 17 and 18 – second body constraint; joints 6, 12 and 19 – the third body constraint. The second body constraint forces the center of the column (i.e., the region where the column is in contact with the beam ends) to have a rigid-body behavior. All three constraints ensure that the sections remain plane along the fiber frame element.

No special link element is used to capture the shear behavior at the beam-column interface, because no shear slip was observed during the test. Therefore, no releases or partial fixity spring were assigned to the beam ends. Moreover, given that L steel profiles used to reinforce the beam ends

(Fig. 3), it is assumed that the stresses in the compressed concrete fibers and the neural axis depth are lower than for monolithic frames. Under these conditions, it is sufficiently accurate to assume that all concrete fibers behave as unconfined concrete through the use of the stress-strain curve presented in Fig. 6(b).

5. Analysis results

Before applying the horizontal displacements, the post-tensioning effect is taken into account by a load case which provides the initial stress conditions for the monotonic and cyclic load cases. The post-tensioning force is simulated by an axial force assigned to the cable element. The results obtained from the analysis are presented in the following section.

5.1 Monotonic behavior

The monotonic force-displacement curve (Fig. 8) is obtained after applying the monotonic loading sequence. In comparison with the loading branch of the positive envelope resulted from the testing program, the analytical model offers a good result (Fig. 8). The two curves almost overlap over the elastic region and nearby the maximum displacement. The horizontal forces that correspond to the maximum drift differ by only $1.69kN$ (i.e., the numerical result is only 1.3% higher than the test result). Moreover, the analytical model shares almost the same initial stiffness as the testing specimen, the differences being lower than 3.5%.

5.2 Cyclic behavior

The cyclic force-displacement curves are obtained after applying the cyclic loading sequence. The analysis results are shown in comparison with the test results in Fig. 9, and their differences regarding the forces at maximum drifts, residual displacements, initial stiffness and interior areas (A_{hy}) are presented in Table 2.

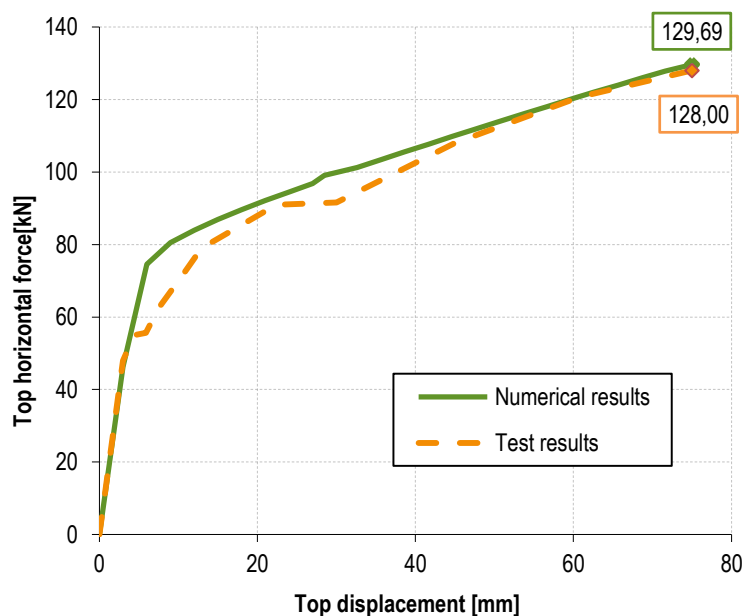


Figure 8. Comparison of monotonic force-displacement curves.

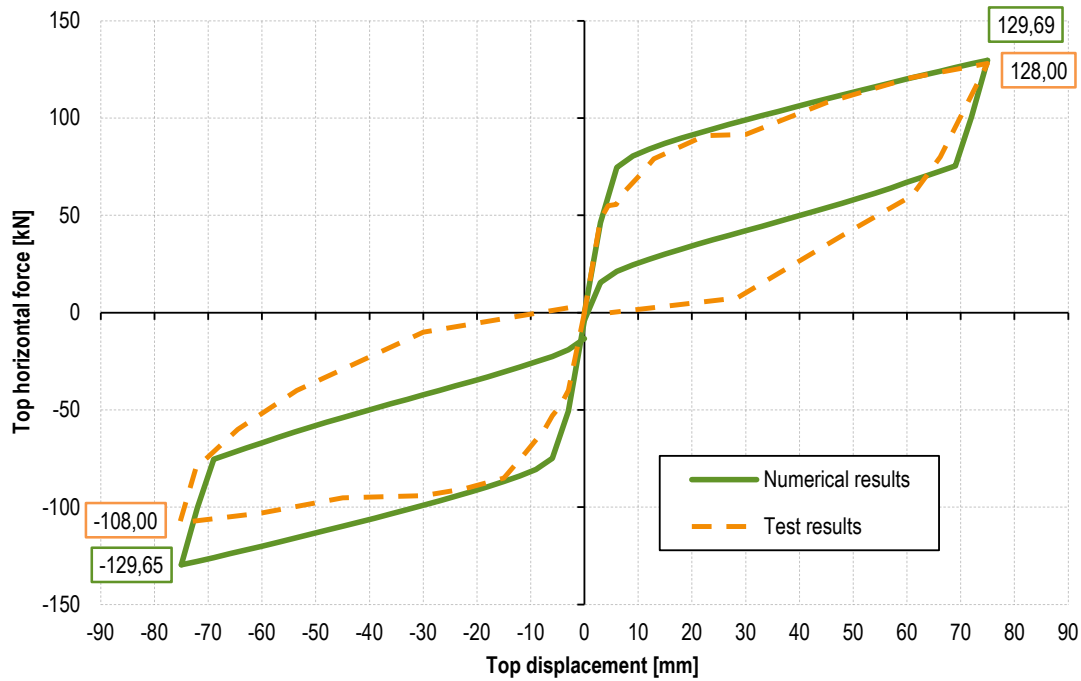


Figure 9. Comparison of cyclic force-displacement curves.

Table 2: Comparison of test and numerical results

| Result provenance | F_{max} | F_{min} | $\Delta_{res} (+)$ | $\Delta_{res} (-)$ | K | K' | A_{hv} |
|--|----------------|------------------|--------------------|--------------------|----------------|----------------|--------------------|
| | [kN] | [kN] | [mm] | [mm] | [kN/mm] | [kN/mm] | [kN·mm] |
| Envelope of hysteresis curves - (Test results) | 128.00 | -108.00 | 4.70 | -8.40 | 16.00 | 13.33 | 9436.38 |
| Cyclic force-displ. curves - (Numerical results) | 129.69 | -129.65 | 0.00 | 0.00 | 15.43 | 15.63 | 7630.59 |
| Differences between numerical and test results | 1.69 (1.3%) | 21.65 (16.7%) | 4.70 (100%) | 8.40 (100%) | 0.57 (3.5%) | 2,3 (14.7%) | 1805.79 (19.1%) |

The results show that the numerical model is unable to represent very accurately the unloading branches of the envelope hysteresis curves and, as a consequence, the self-centering ability is significantly overestimated (i.e., the residual displacements are equal to zero). The loading branches for the negative loading differ considerably, especially at higher drifts, where the differences regarding the horizontal forces reach up to 16.7% (see Table 2). The model considers an almost perfectly symmetrical behavior between the positive and negative loading, while the test results proved the opposite. On the other hand, the estimation of the initial stiffness is sufficiently accurate for both positive and negative loading.

The interior areas of the curves shown in Fig. 9 (i.e., the envelope and cyclic force-displacement curves) differ by 19.1%, the areas of the curves obtained through the numerical analysis being lower. This result is relevant only if the interior areas of the envelope curves can be associated with the energy dissipation capacity of the frame sub-assembly. If so, the analytical model underestimated this aspect.

6. Conclusions

A simple and efficient modeling approach for the nonlinear analysis of an interior precast beam-to-column sub-assembly with hybrid connections is presented. The obtained force-displacement curves are analyzed and compared with both positive and negative envelopes of a similar specimen that was tested at a cyclic loading sequence.

The similarity between the monotonic force-displacement curve obtained from the numerical analysis and the loading branch of the positive envelope curve resulted from the testing program proves that the proposed model is suitable to predict the initial stiffness and the displacement capacity of the test specimen, without the need for any cyclic analysis. However, it seems that the cyclic behavior of the connection is characterized by an asymmetrical response that the analytical model is unable to capture. Moreover, the unloading branches are not properly evaluated through the one-cycle analysis, and more research is needed to capture the self-centering ability and the energy dissipation capacity of the connection.

Acknowledgements

This paper was supported by the project „Doctoral studies in engineering sciences for developing the knowledge based society-SIDOC” contract no. POSDRU/88/1.5/S/60078, project co-funded from European Social Fund through Sectorial Operational Program Human Resources 2007-2013.

7. References

- [1] Stone WC, Cheok GS, Stanton JF. Performance of Hybrid Moment-Resisting Precast Beam-Column Concrete Connections Subjected to Cyclic Loading. *ACI Structural Journal*, Vol. 91(2), pp. 229–249, 1995.
- [2] Priestly MJN, Sritharan S, Conley JR, Pampanin S. Preliminary Results and Conclusions From the PRESSS Five-Story Precast Concrete Test Building. *PCI Journal*, Vol. November-December, pp. 42–67, 1999.
- [3] Hawileh R, Rahman A, and Tabatabai H. Nonlinear finite element analysis and modeling of a precast hybrid beam–column connection subjected to cyclic loads. *Applied Mathematical Modeling*, Vol. 34(9), pp. 2562–2583, 2010.
- [4] Balica NA. *Contributions on improving the theory and practice of reinforced and prestressed concrete buildings*. PhD Thesis, Technical University of Civil Engineering Bucharest, 2010. (in Romanian)
- [5] Priestley MJN, Calvi GM, Kowalsky MJ. *Displacement-Based Seismic Design of Structures*, IUSS Press, Pavia, Italy, 2007.
- [6] ACI Innovation Task Group 1 and Collaborators. *Special Hybrid Moment Frames Composed of Discretely Jointed Precast and Post-Tensioned Concrete Members (ACI T1.2-03) and Commentary (ACI T1.2R-03)*, American Concrete Institute, Farmington Hills, Mich., 2003.
- [7] Faur A, Mircea C. Hybrid connections – the sustainable approach for prefabricated frame structures. In: *Proceedings of Concrete Solutions*, 4th International Conference on Concrete Repair, Grantham M, Mechtcherine V, Schneck U, editors. CRC Press, pp. 227-233, 2011.
- [8] Computers & Structures Inc. *CSI Analysis Reference Manual for SAP2000®, ETABS®, and SAFE*. Berkeley, California, USA, 2011.
- [9] El-sheikh M, Pessiki S, Sause R, Lu L. Moment Rotation Behavior of Unbonded Post-Tensioned Precast Concrete Beam-Column Connections. *ACI Structural Journal*, Vol. 97(1), pp. 122–132, 2000.